THE ASTROPHYSICAL JOURNAL, 493:274–290, 1998 January 20

VLA OBSERVATIONS OF THE SAGITTARIUS D STAR-FORMING REGION

DAVID M. MEHRINGER,[1] W. M. GOSS,[2] D. C. LIS,[1] PATRICK PALMER,[3] AND KARL M. MENTEN[4]
Received 1997 May 8; accepted 1997 August 27

ABSTRACT

We have carried out a program of VLA observations of the Sgr D (G1.13−0.10) star-forming region in order to gain a better understanding of this source. Continuum observations at 6 and 18 cm show a region that is dominated by a single compact source. This source is embedded in a halo of ionized gas and there are several compact continuum sources scattered about the field. The supernova remnant G1.05−0.15 is located 5′ south of the main H II region. From the continuum observations we determined the physical conditions of the thermal sources in Sgr D. Observations of the 6 cm transition of the H_2CO that appears in absorption were also carried out to study the distribution and kinematics of molecular material in this region. These data indicate that the distribution of molecular material is clumpy, with apparent optical depths varying by about 1 order of magnitude within single clouds. In addition, the line widths of the molecular clouds associated with the Sgr D H II region (G1.13−0.10) are ~ 3 km s^{-1}, which is more typical of Galactic disk than Galactic center sources. The narrow molecular lines and the presence of higher velocity, broader H_2CO absorption lines in the Sgr D spectrum indicate that this region is probably located on the far side of the Galactic center region. OH and H_2O maser observations indicate that there may be at least three sites of very recent star formation in this region.

Subject headings: H II regions — ISM: individual: (Sagittarius D) — radio continuum: interstellar — radio lines: ISM

1. INTRODUCTION

The massive star-forming region Sgr D (G1.13−0.10) is a bright radio source with a projected offset of 1° from the Galactic center. Because it is located near the much more prominent sources Sgr A and Sgr B2, which have received considerably more observational attention, relatively little is known about Sgr D. There have been a few previous observations of this region from which a basic picture has developed. Very Large Array[5] (VLA) radio continuum observations have shown that this region is dominated by a single compact source that is surrounded by a halo of diffuse emission (Odenwald 1989; Liszt 1992). In the 18 cm VLA continuum image of Liszt (1992), there are several compact sources in the 36′ field. Also apparent in this image, as well as in the 36 cm image of Gray (1994a) from the Molonglo Observatory Synthesis Telescope, is the supernova remnant (SNR) G1.05−0.15 that is located 5′ to the south of the large Sgr D H II region. However, from previous data it is unclear whether the H II region and SNR are actually located close to one another, or whether their apparent proximity is just a chance projection. The luminosity of the corresponding Sgr D far-infrared source is $6 \times 10^5\ L_\odot$ (Odenwald & Fazio 1984; assuming a distance of 8.5 kpc). Odenwald (1989) has suggested that the morphology of the Sgr D continuum source is consistent with that of a blister H II region. For an expansion velocity of 10 km s^{-1}, the estimated age is 5×10^4 yr. Radio recombination lines observed with the NRAO 43 m telescope show that ionized material in Sgr D has a velocity of −21 km s^{-1} (Anantharamaiah & Yusef-Zadeh 1989). This velocity is forbidden in the sense of Galactic rotation. The associated CS $J = 5 \rightarrow 4$ and $7 \rightarrow 6$ lines have been observed by Lis (1991) using the Caltech Submillimeter Observatory. These lines have velocities of −16 km s^{-1} and are quite narrow (FWHM = 3.7 km s^{-1}). Such narrow lines are commonly observed in Galactic disk star-forming regions. In contrast, the lines in Galactic center molecular clouds are significantly wider (FWHM = 10–20 km s^{-1}; Güsten 1989).

Thus, from these observations it is unclear where Sgr D is located. Based on previous single-dish H_2CO absorption-line studies, Liszt (1992) suggested Sgr D may be located either in or beyond the Galactic center region. On the basis of CS observations, Lis (1991) suggested that this region might be located in the "expanding molecular ring" that is at a distance of 160 pc from the Galactic center.

We have undertaken a program of observations targeting Sgr D in order to gain a better understanding of this region. Using the VLA, we have observed continuum emission from this region at 6 cm and have reprocessed the 18 cm data of Liszt (1992). Continuum observations at these two wavelengths allow for the determination of the radio spectra yielding basic information on the sources in this region. We have also observed the 6 cm ground-state transition of ortho-H_2CO in absorption in order to gain a better picture of the detailed distribution of the molecular gas in this region. In addition, OH and H_2O maser observations were carried out in order to identify sites of very recent star formation.

2. OBSERVATIONS

The 6 cm continuum observations were carried out using the "DnC" configuration of the VLA in 1992 July. This hybrid configuration consists of the southeast and southwest arms in the smallest (D) configuration and the north arm in the larger C configuration. Such a geometry

[1] California Institute of Technology, Downs Laboratory of Physics, MC 320-47, Pasadena, CA 91125.
[2] National Radio Astronomy Observatory, Box O, Socorro, NM 87801.
[3] University of Chicago, Department of Astronomy and Astrophysics, 5640 S. Ellis Ave., Chicago, IL 60637.
[4] Max-Planck-Institut für Radioastronomie, Auf dem Hügel 69, D-53121 Bonn, Germany.
[5] The Very Large Array of the National Radio Astronomy Observatory is a facility of the National Science Foundation operated under cooperative agreement by Associated Universities, Inc.

TABLE 1

PARAMETERS FOR SGR D CONTINUUM OBSERVATIONS

Parameter	Value
VLA configurations	C and D (18 cm)
	DnC (6 cm)
Observing dates	1984 May 19 (C array, 18 cm)
	1984 September 6 (D array, 18 cm)
	1992 July 1 (6 cm)
Total observing time (hr)	7 (C array, 18 cm)
	7 (D array, 18 cm)
	8 (DnC array, 6 cm)
Angular resolution (arcsec)	10 (6 cm)
	15 × 28 ($\alpha \times \delta$) (18 cm)
Primary-beam FWHM (arcmin)	9 (6 cm)
	27 (18 cm)
Pointing position (18 cm)	α(B1950) = 17 45 49.4, δ(B1950) = −27 53 48
Pointing positions (6 cm)	α(B1950) = 17 45 38.0, δ(B1950) = −28 05 00
	α(B1950) = 17 45 22.0, δ(B1950) = −28 05 00
	α(B1950) = 17 45 25.0, δ(B1950) = −28 00 00
	α(B1950) = 17 45 15.0, δ(B1950) = −27 56 00
	α(B1950) = 17 45 36.0, δ(B1950) = −27 54 00

NOTE.—Units of right ascension are hours, minutes, and seconds, and units of declination are degrees, arcminutes, and arcseconds.

produces a circular beam for sources south of $\delta = -15°$. Five 6 cm continuum fields were observed. A typical resolution was 10″ for the uniformly weighted 6 cm continuum images. The 18 cm continuum observations were carried out by Liszt (1992) using the C and D configurations of the VLA. The maximum resolution of these images was 28″ × 15″ (P.A. = −7°). Other relevant parameters for the continuum observations are summarized in Table 1.

The 6 cm H_2CO observations were carried out using the DnC configuration in July 1992. A single field was observed and the naturally weighted channel images had an angular resolution of 13″. The H_2CO observation used the 4IF mode of the VLA correlator. The two IF pairs were centered at +54 and −34 km s^{-1}. In addition, within both IF pairs, one IF had a total bandwidth of 3.125 MHz (195 km s^{-1}) and 31 Hanning-smoothed channels giving a spectral resolution of 97.7 kHz (6.0 km s^{-1}). The other IF within the pair had a total bandwidth of 1.5625 MHz (100 km s^{-1}) and 63 Hanning-smoothed channels for a spectral resolution of 24.4 kHz (1.5 km s^{-1}). Thus, the LSR velocity range of −130 to +150 km s^{-1} was covered with 6.0 km s^{-1} spectral resolution and the LSR velocity range of −90 to +100 km s^{-1} was covered with 1.5 km s^{-1} spectral resolution. Other relevant H_2CO observational parameters are summarized in Table 2.

The OH maser observations were carried out at the OH transition frequencies of 1612, 1665, and 1667 MHz so that we could distinguish between maser emission associated with evolved stars or young stellar objects. A single field was observed using the BnA configuration. Both left and right circularly polarized radiation was observed. The observing band was centered at −15 km s^{-1} and had a total bandwidth of 1.5625 MHz (280 km s^{-1}). This spectral window was divided into 127 Hanning-smoothed channels producing a spectral resolution of 12.2 kHz (2.2 km s^{-1}). Other relevant parameters for the OH maser observations are summarized in Table 3.

The H_2O maser observations were carried out using the DnC configuration and two fields were observed. These observations were part of a project to search for masers in several regions near the Galactic center; the results for other regions will be discussed in a future publication (Lis, Menten, & Mehringer 1998). Two spectral windows that have center velocities of −45 and +15 km s^{-1} were observed simultaneously. Each window had a total bandwidth of 6.25 MHz (90 km s^{-1}) and was divided into 63 non–Hanning-smoothed channels for a nominal spectral resolution of 97.7 kHz (1.3 km s^{-1}). During postprocessing, the data were Hanning smoothed, and so the spectral resolution decreased to twice its nominal value. Other rele-

TABLE 2

PARAMETERS FOR SGR D H_2CO OBSERVATIONS

Parameter	Value
VLA configuration	DnC
Observing date	1992 July 2
Total observing time (hr)	8
Angular resolution (arcsec)	13
Primary-beam FWHM (arcmin)	9
Pointing position	α(B1950) = 17 45 25.0, δ(B1950) = −28 00 00
H_2CO 1_{10}–1_{11} rest frequency (MHz)	4829.6594
Spectrometer configuration	63/31 frequency channels
	1.5625/3.125 MHz IF bandwidth
	24/97 kHz (1.5/6.0 km s^{-1}) channel width
	IF pairs centered at −33.9 and +53.9 km s^{-1}
	On-line Hanning smoothing

NOTE.—Units of right ascension are hours, minutes, and seconds, and units of declination are degrees, arcminutes, and arcseconds.

TABLE 3

PARAMETERS FOR SGR D OH MASER OBSERVATIONS

Parameter	Value
VLA configuration	BnA
Observing date	1993 February 14
Total observing time (hr)	3
Angular resolution (arcsec)	6×4 (P.A. = 20°)
Primary-beam FWHM (arcmin)	27
Pointing position	α(B1950) = 17 45 30 0, δ(B1950) = −28 00 40
OH $^2\Pi_{3/2}$ $J = 3/2$, $F = 1$–2 rest frequency (MHz)	1612.2310
OH $^2\Pi_{3/2}$ $J = 3/2$, $F = 1$–1 rest frequency (MHz)	1665.4018
OH $^2\Pi_{3/2}$ $J = 3/2$, $F = 2$–2 rest frequency (MHz)	1667.3590
Spectrometer configuration	Simultaneous observations of right circular polarization and left circular polarization radiation 127 frequency channels 1.5625 MHz IF bandwidth 12 kHz (2.2 km s^{-1} at 1665 MHz) channel width IF pair centered at −15 km s^{-1} On-line Hanning smoothing

NOTE.—Units of right ascension are hours, minutes, and seconds, and units of declination are degrees, arcminutes, and arcseconds.

vant parameters for the H_2O maser observations are summarized in Table 4.

3. RESULTS AND DISCUSSION

3.1. *Radio Continuum Observations*

The primary objective of the continuum study was to image the ionized gas in Sgr D at 6 and 18 cm. From these data, the spectra and physical conditions of the sources can be determined. Like previous continuum images of this region, our images show that Sgr D is dominated by a single compact source (source 3 of Liszt 1992 [G1.12−0.10]) that is embedded in a halo of diffuse emission. There are also a number of compact sources scattered about the field. Figure 1 is an 18 cm contour image of the Sgr D region. This image was created using both C- and D-configuration data and has a resolution of $28'' \times 15''$ (P.A. = −7°). The source designations of Liszt (1992) are used. The flux density of all sources in the field, including the emission regions in the northeast and northwest portions of Figure 1, is about 25 Jy. Figure 2 is a 6 cm contour image of the Sgr D region. This image is a five-field mosaic and has a resolution of 10″.

The 6 and 18 cm flux densities of the large Sgr D H II region (G1.13−0.10) are 9.5 and 14.5 Jy, respectively. Some emission at 6 cm was not detected because of missing short antenna spacings that correspond to fringe spacings of $\gtrsim 5'$. Assuming that the 18 and 6 cm flux densities are equal, which is expected for an optically thin, thermal source, this undetected component has a 6 cm flux density of 5 Jy.

The SNR G1.05−0.15 is located 5′ south of the H II region. It is brightened on the northern edge. The SNR flux densities at 6 and 18 cm are 5.0 and 12.3 Jy, respectively. Although some of the emission was probably not recorded at 6 cm because of the missing short spacings, the rising flux density of this source at longer wavelengths is also due to its nonthermal nature; Gray (1994a) reports a 36 cm flux density of 18 Jy.

In addition to the Sgr D H II region (G1.13−0.10) and the G1.05−0.15 SNR, the extended emission region G1.4−0.1 is apparent about 15′ northeast of Sgr D (G1.13−0.10) in Figure 1. Gray (1994b) has suggested that this region may be an SNR. In the 18 cm image presented here, it has a flux density of about 4 Jy.

The observed parameters for the compact sources are presented in Table 5. Listed in this table are the source designation, the peak position, the 6 and 18 cm flux densities ($S_{6\ \mathrm{cm}}$, $S_{18\ \mathrm{cm}}$), and the FWHM diameter of the source. Sources that have flux density measurements at both 6 and 18 cm probably have thermal spectra. Source 5 has a greater flux density at 18 cm than at 6 cm. However, this

TABLE 4

PARAMETERS FOR SGR D H_2O MASER OBSERVATIONS

Parameter	Value
VLA configuration	DnC
Observing date	1993 January 31
Total observing time (hr)	1
Angular resolution (arcsec)	3
Primary-beam FWHM (arcmin)	2
Pointing positions	α(B1950) = 17 45 32.0, δ(B1950) = −28 00 45 α(B1950) = 17 45 24.0, δ(B1950) = −28 01 35
H_2O $6_{1,6}$–$5_{2,3}$ rest frequency (MHz)	22235.08
Spectrometer configuration	63 frequency channels 6.25 MHz IF bandwidth 98 kHz (1.3 km s^{-1}) channel width IF pairs centered at −45 and +15 km s^{-1} No on-line Hanning smoothing, data smoothed off line

NOTE.—Units of right ascension are hours, minutes, and seconds, and units of declination are degrees, arcminutes, and arcseconds.

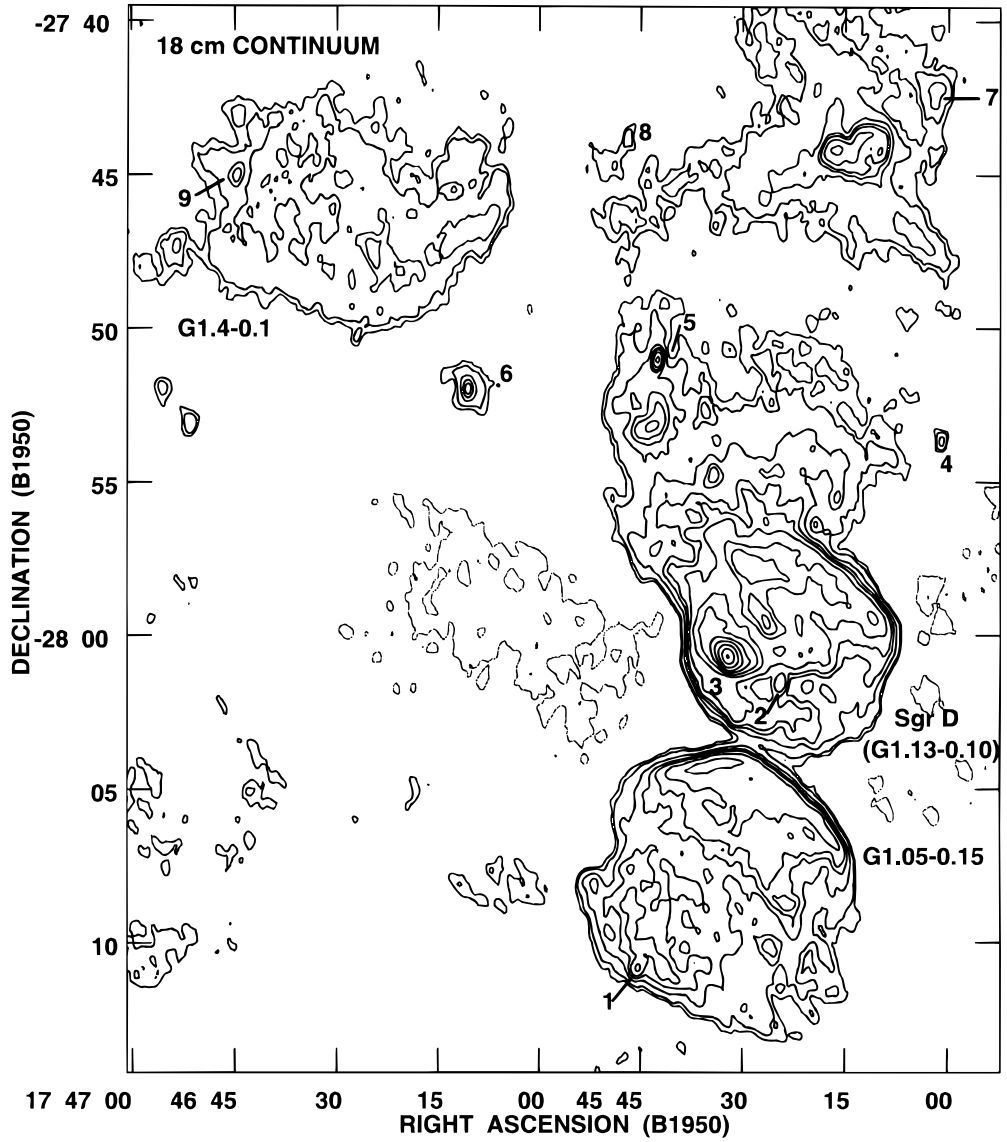

FIG. 1.—An 18 cm continuum image of the Sgr D region created from the C- and D-configuration data of Liszt (1992). The resolution is 28″ × 15″ (P.A. = −6.8°). Contour levels are at −10, 3, 5, 10, 15, 20, 30, 50, 70, 100, 150, 250, 450, and 750 mJy beam^{-1}. The rms noise is 2 mJy beam^{-1} and the image has not been corrected for primary-beam attenuation.

source is embedded in a low-intensity extended component, making flux density measurements difficult. Because of the relatively coarse resolution (10″) of these observations, most of the compact sources are unresolved.

TABLE 5

OBSERVATIONAL PARAMETERS OF CONTINUUM SOURCES IN SGR D

Source	α(B1950)	δ(B1950)	$S_{6\ cm}$ (mJy)	$S_{18\ cm}$ (mJy)	FWHM (arcsec)
1a.....	17 45 46.2	−28 11 03	17	...	<10
1b.....	17 45 45.3	−28 10 57	33	...	<10
2	17 45 24.4	−28 02 35	60	30	≤10
3	17 45 32.2	−28 00 44	2300	1900	20 × 10
4	17 45 01.0	−27 53 42	33	12	<10
5	17 45 42.4	−27 51 02	17	46	<10
6	17 46 10.5	−27 51 58	...	51	<15
7	17 45 01.6	−27 42 11	...	160	~50 × 75
9	17 46 44.6	−27 45 01	...	47	≤15
10.....	17 45 15.0	−27 51 27	11	...	<10

NOTE.—Units of right ascension are hours, minutes, and seconds, and units of declination are degrees, arcminutes, and arcseconds.

Physical parameters for the H II regions listed in Table 5 are presented in Table 6. In this table the source designation, the peak emission measure (Peak EM), the rms electron number density (rms n_e), the mass of the ionized material ($M_{H\ II}$), the logarithm of the number of ionizing

TABLE 6

DERIVED PHYSICAL PARAMETERS OF CONTINUUM SOURCES IN SGR D

Source	Peak EM (10^6 cm^{-6} pc)	rms n_e (10^3 cm^{-3})	$M_{H\ II}$ ($M_\odot$)	log N_i (photons s^{-1})	ZAMS
1a.....	0.09	>0.5	<1.5	47.1	B0
1b.....	0.08	>0.4	<2.1	47.4	B0
2	0.08	≥0.4	≤2.8	47.7	O9.5
3	2.1	1.9	29	49.2	O5.5
4	0.11	>0.5	<2.1	47.4	B0
5	0.06	>0.4	<1.5	47.1	B0
6	0.02	>0.2	<4.5	47.5	B0
7	0.02	0.1	...	48.0	O9
9	0.03	>0.2	<4.3	47.5	B0
10.....	0.04	>0.3	<1.2	46.9	B0

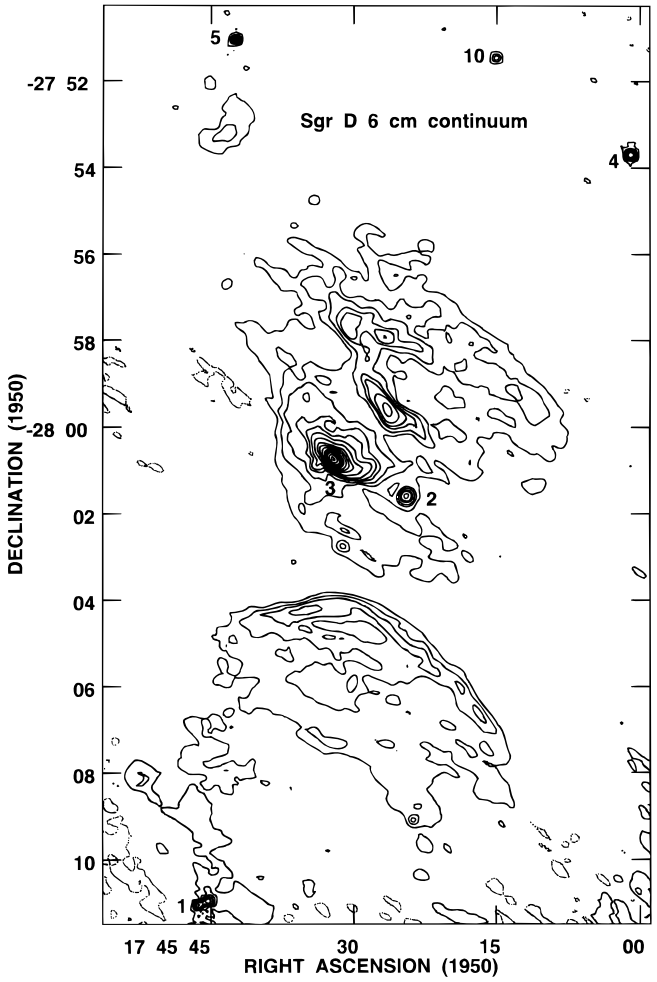

FIG. 2.—A 6 cm, five-field mosaic of Sgr D. The image was created using VTESS, an Astronomical Image Processing System (AIPS) maximum entropy deconvolution routine. The resolution is 10.3″ × 9.7″ (P.A. = 82°). Contours are at −2, 2, 5, 8, 12, 15, 20, 30, 50, 70, 100, 150, 200, 250, and 300 mJy beam^{-1}. The rms noise near the center of the image is 0.5 mJy beam^{-1}, and the primary-beam response for each field has been taken into account during mosaicking.

photons (N_i), and the spectral type of a single zero-age main sequence star (ZAMS) that would ionize the gas are listed. An electron temperature of 7,000 K and a distance of 8.5 kpc were assumed for all sources. While we have adopted the distance to the Galactic center for the distance to Sgr D, it should be kept in mind that Sgr D may be located significantly farther than this distance (see below).

Peak emission measures and electron densities were computed using the methods of Wood & Churchwell (1989). Masses were computed for unresolved sources assuming that they are spherical. The number of ionizing photons was computed for all sources using the equations of Mezger & Henderson (1967), the refinements of Panagia & Walmsley (1978), and corrections to the latter paper made by F. Vial-lefond (1991, private communication). The ZAMS star was determined using the data of Panagia (1973). In the case of unresolved sources, the listed emission measure and electron density are lower limits, while the mass of ionized gas is an upper limit.

Like Sgr B (e.g., Mehringer et al. 1992), Sgr D has a halo of extended emission. The average 18 cm intensity of this component corresponds to an emission measure of 4×10^4 cm^{-6} pc. For a diameter of 7′ (17 pc), the rms electron density is ~ 50 cm^{-3}. The mass of the ionized gas in this component is $\sim 3000\ M_\odot$. These parameters are similar to those found for Sgr B1 and Sgr B2 (Mehringer et al. 1992, 1993b). In the case of Sgr B1, the associated extended component has an rms electron number density of 80 cm^{-3}, and the mass of ionized material is 5000 $M_\odot$ (Mehringer et al. 1992). In the case of Sgr B2, these parameters are 60 cm^{-3} and 3000 $M_\odot$, respectively (Mehringer et al. 1993b).

Odenwald & Fazio (1984) have estimated the luminosity of Sgr D to be $6(\pm 5) \times 10^5\ L_\odot$ based on far-IR measurements. This luminosity is low compared to the radio flux density of 14.5 Jy, assuming that all the radio continuum flux is produced by material that is ionized by stars. A single star of spectral type O4 would be sufficient to ionize the gas. However, this star would have a total luminosity of $1.2 \times 10^6\ L_\odot$, twice that estimated by Odenwald & Fazio (1984; although marginally consistent with their uncertainty). However, if the initial mass function (IMF) of stars in Sgr D is similar to the solar neighborhood IMF, then in order to produce the observed radio continuum flux density, the total luminosity of stars in the region would be $\sim 3 \times 10^6\ L_\odot$, about 6 times the value determined by Odenwald & Fazio (1984). The low luminosity of Sgr D as determined from the far-IR data may indicate that there is not enough dust in the immediate vicinity to absorb and reemit all of the stellar radiation, or that the IMF in Sgr D significantly differs from that in the solar neighborhood.

3.2. 6 cm H_2CO *Absorption Observations*

The H_2CO absorption study was difficult because of the low optical depths toward Sgr D and the low continuum intensities. In addition, the complicated morphology of this region often caused the spectra to have nonlinear baselines, which made it difficult to identify weak lines. A continuum image produced from line-free channels is shown in Figure 3. The letters mark the positions where H_2CO spectra were taken. The narrowband (1.5625 MHz bandwidth) spectra are displayed in Figure 4*a* and the wide-band (3.125 MHz bandwidth) spectra are presented in Figure 4*b*. One or more Gaussians were fitted to the narrowband spectra and the results are presented in Table 7. Listed in this table are the source designation, the central position, the mean 6 cm continuum intensity ($\overline{I}_c$), the dimensions of the rectangular area over which the spectrum was integrated, the line central velocity ($v_{\rm LSR}$), the line FWHM (Δv), the optical depth at line center (τ_0), and the ratio of the column density of H_2CO in the lower state to the excitation temperature ($N_L/T_{\rm ex}$). This last quantity was calculated using

$$\frac{N_L}{T_{\rm ex}} = 1.36 \times 10^{13} \tau_0\, \Delta v\ , \qquad (1)$$

where $N_L/T_{\rm ex}$ has units of cm^{-2} K^{-1}, and Δv, the FWHM of the assumed Gaussian-shaped line profile, has units of km s^{-1}. Because of the low spectral resolution and narrow line widths, fits were not made for the wide-band spectra.

Position A corresponds to source 3 (G1.12−0.10) of the continuum study. Because this source is relatively intense, lines with low optical depths (<0.10) could be observed. There are four lines for which good fits were obtained (see Table 7). The three lines at negative velocities are narrow ($\Delta v < 5$ km s^{-1}) and the optical depths for all these lines are small (<0.3). The H_2CO absorption feature at −17.1 km

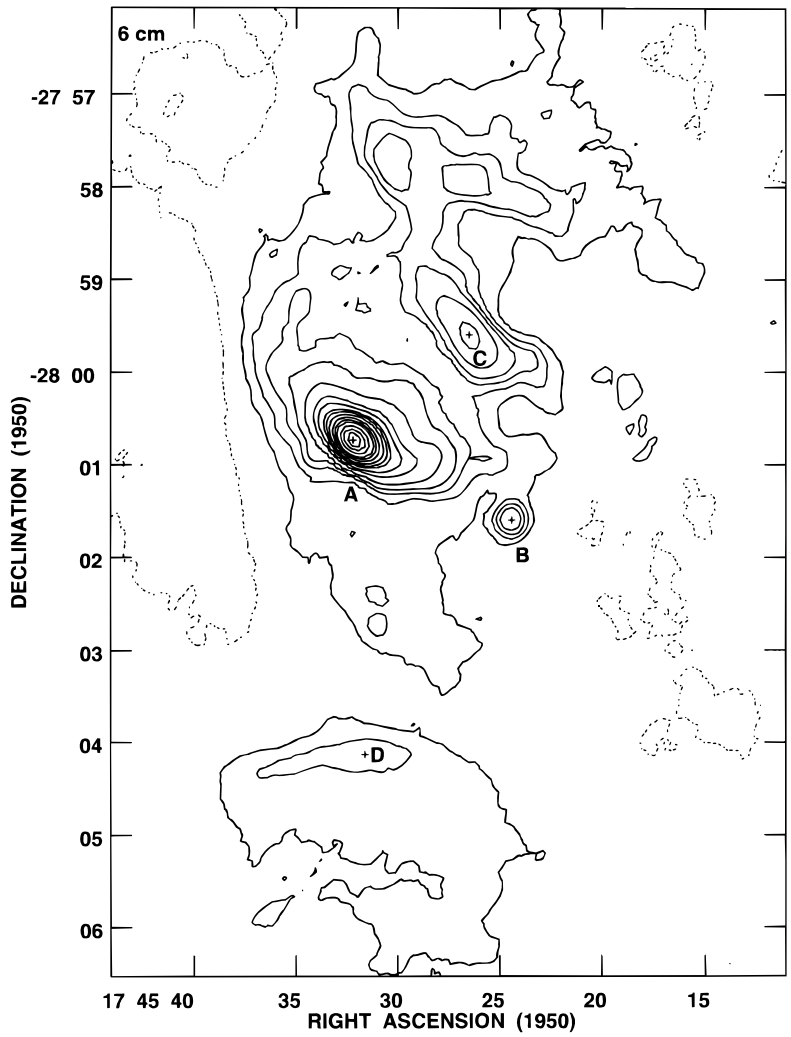

FIG. 3.—A 6 cm continuum image produced from line-free channels of the H_2CO data. The resolution is 13″ × 12″ (P.A. = −33°). Contours are at −5, 5, 10, 15, 20, 30, 50, 70, 100, 120, 150, 200, 250, 300, 400, 500, and 600 mJy beam^{-1}. The image has not been corrected for primary-beam attenuation. The crosses mark the positions at which the H_2CO spectra displayed in Fig. 4 were determined.

s^{-1} is very likely to be due to the molecular cloud associated with the Sgr D H II region (G1.13−0.10); the ionized material has a velocity of −21 km s^{-1} (Anantharamaiah & Yusef-Zadeh 1989).

Position B includes source 2 (G1.10−0.09) of the continuum study. As at position A, the line widths for the clouds at negative velocities are less than 5 km s^{-1}. Because of the low continuum intensity, only clouds with optical depths $\gtrsim 0.4$ could be detected. The $v_{LSR} = -18.1$ km s^{-1} line at position B and the $v_{LSR} = -17.1$ km s^{-1} line at position A are probably due to the same cloud. The difference in velocities represents a gradient of 0.21 km s^{-1} pc^{-1}. The difference in optical depth is about a factor of 10, indicating that this feature is quite nonuniform. Similarly, the −14.5 km s^{-1} line at position B and the −11.3 km s^{-1} line at position A may be due to the same feature. The gradient in this case is 0.68 km s^{-1} pc^{-1}, and the optical depth difference from position B to position A is about a factor of 2.5.

Position C is located in the wishbone-shaped region located north of position A. There is only one certain line detection at this position, at −19.6 km s^{-1}. This line and the −17.1 km s^{-1} line at position A are probably due to the same feature. The velocity gradient between positions A and C is 0.60 km s^{-1} pc^{-1}.

Position D is located in the brightest part of the SNR. Unlike the other three positions, no lines are detected near $v_{LSR} = -18$ km s^{-1}.

Optical depth spectra made by averaging over the entire Sgr D H II region (G1.13−0.10) are displayed in Figure 5, and similar spectra for the G1.05−0.15 SNR are displayed in Figure 6. Because of the complexity of the narrowband spectra and the low spectral resolution of the wide-band spectra, attempts to fit Gaussians to these spectra were unsuccessful in most cases.

Downes et al. (1980) included Sgr D (G1.13−0.10) and the G1.05−0.15 SNR in their H_2CO and H110α recombination-line survey of Galactic radio sources using the Effelsberg 100 m telescope. A comparison between central velocities of features observed in their study and the present investigation is given in Table 8. For the most part, there is good correspondence between spectral features observed with the 100 m telescope and those observed with the VLA. One notable exception is in the +40 to +90 km s^{-1} range toward the Sgr D H II region (G1.13−0.10). However, from the 6 cm H_2CO spectrum of Wadiak, Rood, & Wilson (1988) a single, broad absorption feature is quite apparent in this velocity range. This feature is most likely the result of a superposition of several clouds, and so veloc-

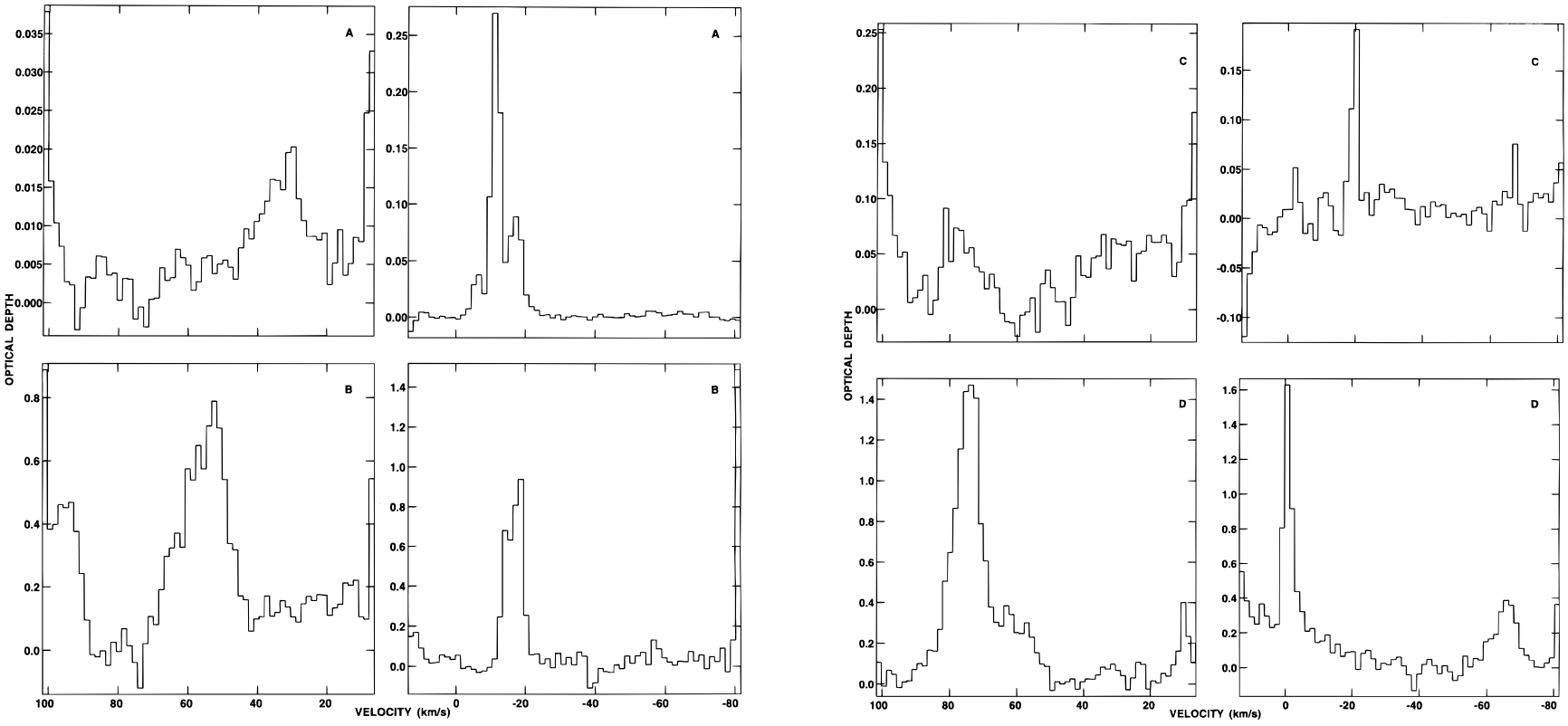

FIG. 4*a*

FIG. 4.—H_2CO apparent optical depth spectra taken at selected positions labeled in Fig. 3. (*a*) Narrow (1.5625 MHz) bandwidth spectra. The channel width is 1.5 km s^{-1}. (*b*) Wide (3.125 MHz) bandwidth spectra. The channel width is 6.0 km s^{-1}. Note that the two narrow bandwidth as well as the two wide bandwidth spectra at all positions partially overlap in velocity.

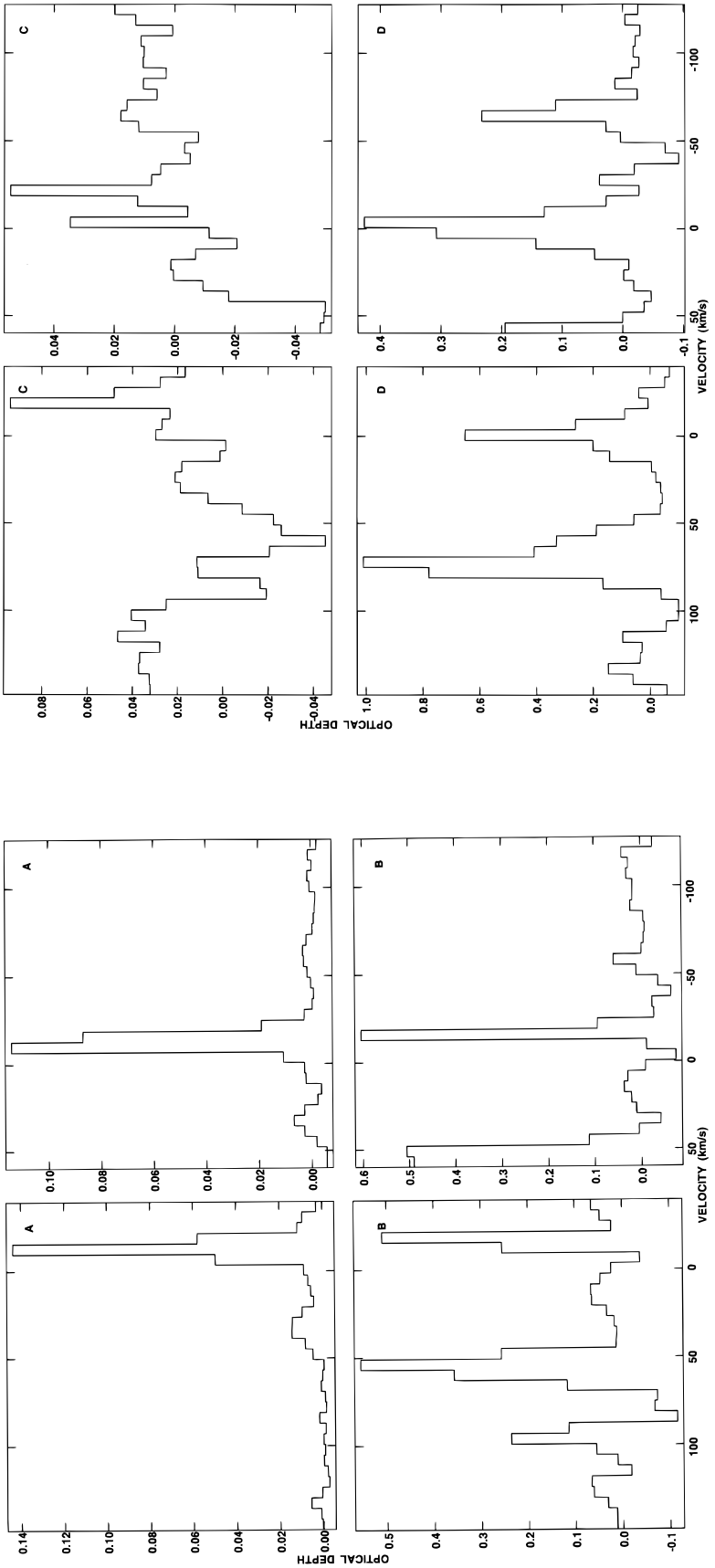

FIG. 4*b*

TABLE 7

H_2CO Parameters for Positions in Sgr D

Source	α	δ	T_c (mJy beam^{-1})	Box Size (arcsec)	v_{LSR}[a] (km s^{-1})	Δv[a] (km s^{-1})	τ_0[a]	N_L/T_{ex}[a] (10^{13} cm^{-2} K^{-1})
A	17 45 32.2	−28 00 44	440	20 × 20	−17.1 (0.1)	4.3 (0.2)	0.092 (0.004)	0.54 (0.03)
					−11.3 (0.1)	3.0 (0.2)	0.276 (0.005)	1.13 (0.08)
					−6.0 (0.1)	3.0 (0.3)	0.039 (0.005)	0.16 (0.03)
					+32.7 (0.6)	18.0 (1.5)	0.013 (0.002)	0.32 (0.06)
B	17 45 24.4	−28 01 36	23	12 × 12	−18.1 (0.1)	2.8 (0.2)	1.0 (0.1)	3.8 (0.5)
					−14.5 (0.1)	3.1 (0.3)	0.7 (0.1)	3.0 (0.5)
					+54.9 (0.4)	14 (1)	0.63 (0.07)	12 (2)
					+95.8 (0.6)	8 (2)	0.4 (0.1)	4.4 (1.5)
C	17 45 26.5	−27 59 36	45	20 × 20	−19.6 (0.1)	2.0 (0.5)	0.21 (0.05)	0.6 (0.2)
D	17 45 31.6	−28 04 08	10	68 × 20	65.6 (0.7)	7 (2)	0.28 (0.09)	3 (1)
					−0.8 (0.2)	5.1 (0.4)	1.0 (0.1)	6.9 (0.9)
					+59.8 (0.4)	9 (1)	0.29 (0.05)	3.5 (0.7)
					+74.6 (0.1)	10.6 (0.2)	1.41 (0.04)	20.3 (0.7)

Note.—Units of right ascension are hours, minutes, and seconds, and units of declination are degrees, arcminutes, and arcseconds.
[a] Values in parentheses are the uncertainties.

ity assignments of individual components are somewhat subjective. This is especially true for the 100 m measurements, because the angular resolution is very coarse at 2.6′.

Results of recent studies (e.g., Lis 1991) indicate that Sgr D is not located in the Galactic center region. The CS line that has a velocity near the recombination-line velocity has a width of only 3.7 km s^{-1}. Such narrow molecular lines are typical of Galactic disk molecular clouds. In contrast, Galactic center molecular clouds usually have much wider lines, in the range of 10–20 km s^{-1}. The present H_2CO study supports the view that Sgr D is not located in the Galactic center region. The line width of the absorption feature observed near −18 km s^{-1} is narrow with widths ranging from 2 to 4 km s^{-1}.

Having determined that Sgr D is not located in the Galactic center region, the question of whether Sgr D is located on the near or far side of the Galactic center remains. The H_2CO spectrum of region B and the H_2CO spectrum of the entire Sgr D H II region (G1.13−0.10) display significant absorption near +50 km s^{-1}. This feature is probably due to a Galactic center cloud for the following reasons: (1) the width is significantly greater than 10 km s^{-1}, and (2) the feature is not near 0 km s^{-1}, as would be expected if it were located in the Galactic disk at this Galactic longitude. Because H_2CO in this cloud is observed in absorption toward the Sgr D H II region (G1.13−0.10), Sgr D is probably located beyond the Galactic center. It is to be noted that, if Sgr D is indeed located on the far side of

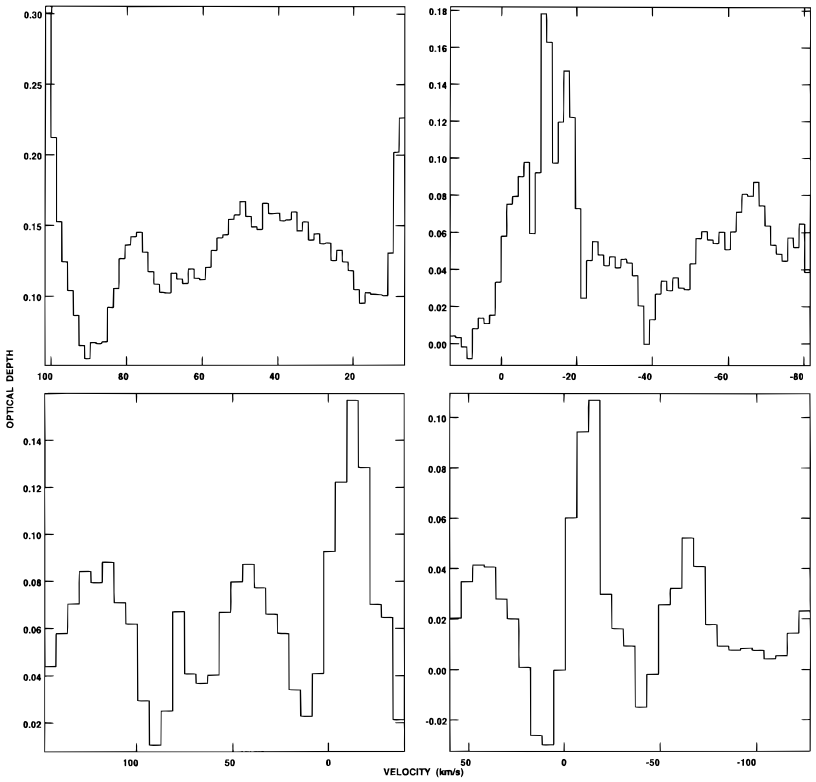

Fig. 5.—H_2CO spectra from each of the 4 IFs produced by averaging over the entire Sgr D H II region (G1.13−0.10). Note that the two narrow bandwidth as well as the two wide bandwidth spectra partially overlap in velocity.

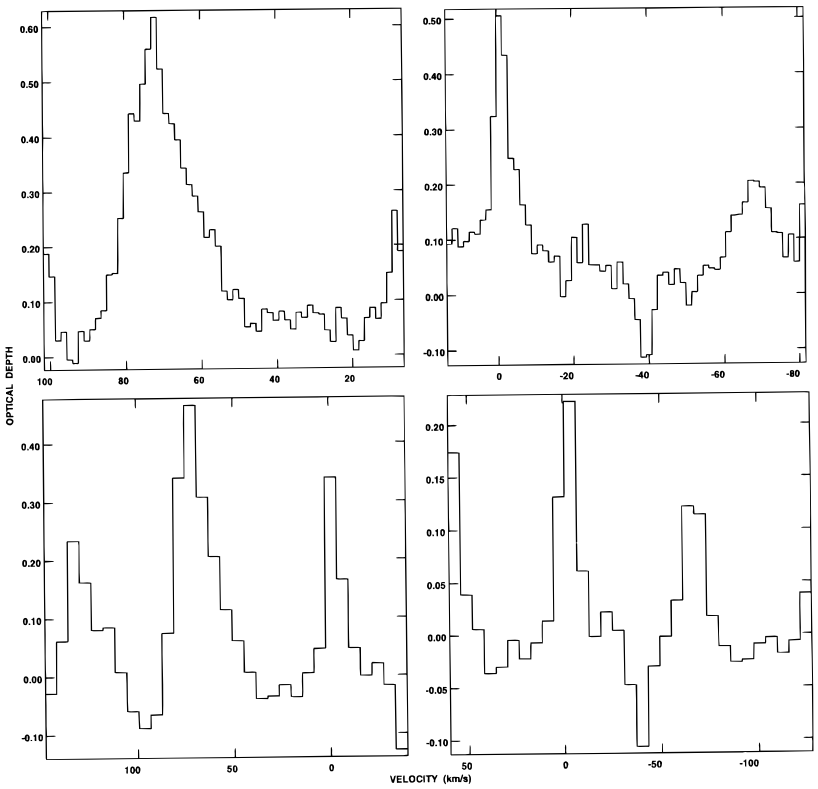

FIG. 6.—Same as Fig. 5, but for G1.05 − 0.15 SNR

the Galactic center, the number of Lyman continuum photons (which scales as D^2) and the ZAMS listed in Table 7 represent lower limits, because the distance used in calculating these parameters was taken to be 8.5 kpc, the distance of the Galactic center.

The H_2CO spectrum of the SNR G1.05 − 0.15 also displays absorption near +50 km s^{-1}, indicating that it, too, lies beyond the Galactic center. However, unlike the Sgr D H II region (G1.13 − 0.10), no absorption was detected in the SNR spectrum near −18 km s^{-1}. On the other hand, the single-dish observation of Downes et al. (1980) did detect absorption at −16 km s^{-1} with $\tau_0 = 0.07$, which is below the detection limit of the present study. Therefore, based on previous data, it appears that the SNR G1.05 − 0.15 is at least as distant as the H II region Sgr D (G1.13 − 0.10).

TABLE 8

COMPARISON OF VLA AND BONN H_2CO LINE-CENTER VELOCITIES[a]

Source	Bonn (km s^{-1})	VLA (km s^{-1})
Sgr D.....	−64.0	−65(2)
	−17.0	−17.1(1.5)[b]
	−11.0	−11.0(1.5)[b]
	−5.0	−6.5(1.5)[b]
	...	+41.7(0.7)
	...	+78.4(0.4)
	+84.0	...
	+123.0	+115(6)[b]
G1.05.....	...	−67.8(0.9)
	−16.0	...
	−1.0	−1.2(0.3)
	+71.0	+71.4(0.3)
	+125	+129(2)

[a] Uncertainties in the Bonn center velocities are ±0.5 km s^{-1}.

[b] Gaussian fit failed. Velocity refers to channel containing local maximum, and the uncertainty is equal to the channel width.

3.3. OH *and* H_2O *Masers*

As discussed in § 2, OH maser observations at 1612, 1665, and 1667 MHz were carried out so that we could distinguish between masers associated with evolved stars and those associated with young stellar objects, and hence, sites of very recent star formation. Sources displaying 1612 MHz double-peaked spectral profiles are almost always associated with evolved stars (Wilson & Barrett 1972; Likkel 1989). The typical separation of the peaks in 1612 MHz spectra of evolved stars is 30 km s^{-1}; the great majority are between 20 and 40 km s^{-1} (te Lintel Hekkert et al. 1989). We have detected 14 OH maser sites in the field near the Sgr D H II region (G1.13 − 0.10).

The observational parameters of these masers are summarized in Table 9, in which a channel-by-channel listing of maser emission is presented. Listed in this table are the maser designation, the position, transition (1612, 1665, or 1667 MHz), sense of circular polarization, velocity of the channel in which emission occurs (v_{LSR}), and flux density of the emission in that channel. In Figure 7, the positions of the OH maser sites are superposed on the 18 cm continuum image. In addition, the positions of two 1720 MHz OH masers (labeled Z1 and Z2) detected by Yusef-Zadeh et al. (1998) are also indicated in this figure. The spectra of all the OH masers are displayed in Figure 8. In addition, two H_2O maser sites were detected, and their parameters are summarized in Table 10, which has a similar format to Table 9 (with the exception that polarization information is not listed because H_2O masers are not polarized). In Figure 9,

TABLE 9

OBSERVATIONAL PARAMETERS OF OH MASERS TOWARD SGR D[a]

Source	α(B1950)	δ(B1950)	Transition (MHz)	Circular Polarization	v_{LSR} (km s^{-1})	Flux Density (mJy)
A	17 44 31.23 (0.02)	−28 10 37.9 (0.5)	1667	L	+104	130
			1667	R	+104	170
B	17 44 37.93 (0.02)	−27 51 38.0 (0.5)	1612	L	+53	180
			1612	L	+55	270
			1612	L	+85	130
			1612	L	+87	150
			1612	R	+53	180
			1612	R	+55	310
			1612	R	+85	150
			1612	R	+87	170
C	17 44 46.37 (0.03)	−28 05 31.4 (0.6)	1612	L	+37	90
			1612	L	+40	210
			1612	L	+42	60
			1612	L	+69	80
			1612	L	+71	140
			1612	R	+37	100
			1612	R	+40	210
			1612	R	+42	50
			1612	R	+69	90
			1612	R	+71	130
D.....	17 44 53.20 (0.09)	−27 48 25.3 (0.8)	1612	L	+15	90
			1612	R	+15	100
E	17 45 05.11 (0.04)	−28 07 55.2 (0.5)	1667	L	+75	100
			1667	L	+77	70
			1667	R	+75	90
			1667	R	+77	50
F	17 45 13.96 (0.07)	−28 19 22.3 (0.6)	1612	L	+62	210
			1612	L	+98	140
			1612	L	+101	130
			1612	R	+62	220
			1612	R	+98	180
			1612	R	+101	200
G.....	17 45 18.15 (0.02)	−27 56 52.0 (0.4)	1612	L	−63	480
			1612	L	−60	430
			1612	L	−45	80
			1612	L	−42	330
			1612	L	−40	1030
			1612	L	−38	70
			1612	R	−63	500
			1612	R	−60	430
			1612	R	−45	80
			1612	R	−42	370
			1612	R	−40	1090
			1612	R	−38	80
			1665	L	−61	110
			1665	L	−59	130
			1665	L	−57	70
			1665	L	−48	120
			1665	L	−46	160
			1665	L	−44	<60
			1665	R	−61	150
			1665	R	−59	140
			1665	R	−57	<50
			1665	R	−48	80
			1665	R	−46	160
			1665	R	−44	70
			1667	L	−63	60
			1667	L	−61	160
			1667	L	−59	160
			1667	L	−57	60
			1667	L	−48	70
			1667	L	−46	230
			1667	L	−44	250
			1667	L	−41	50
			1667	R	−63	60
			1667	R	−61	160
			1667	R	−59	160
			1667	R	−57	60
			1667	R	−48	70
			1667	R	−46	230
			1667	R	−44	250
			1667	R	−41	50

TABLE 9—*Continued*

Source	α(B1950)	δ(B1950)	Transition (MHz)	Circular Polarization	v_{LSR} (km s^{-1})	Flux Density (mJy)
H	17 45 23.01 (0.01)	−27 59 00.0 (0.2)	1612	L	+37	430
			1612	L	+40	170
			1612	L	+62	<50
			1612	L	+64	200
			1612	R	+37	420
			1612	R	+40	160
			1612	R	+62	40
			1612	R	+64	240
I	17 45 39.25 (0.02)	−28 00 15.1 (0.1)	1665	L	−22	50
			1665	L	−19	130
			1665	L	−17	40
			1665	R	−22	<40
			1665	R	−19	<40
			1665	R	−17	<40
J	17 45 40.59 (0.04)	−28 13 31.2 (0.3)	1612	L	−17	140
			1612	L	−15	160
			1612	L	−13	60
			1612	L	+15	80
			1612	L	+17	100
			1612	L	+19	170
			1612	L	+21	200
			1612	R	−17	110
			1612	R	−15	150
			1612	R	−13	90
			1612	R	+15	90
			1612	R	+17	90
			1612	R	+19	150
			1612	R	+21	190
K	17 45 45.74 (0.04)	−28 10 52.2 (0.4)	1665	L	0	120
			1665	L	+3	270
			1665	L	+5	<40
			1665	L	+7	<40
			1665	R	0	<40
			1665	R	+3	70
			1665	R	+5	70
			1665	R	+7	70
L	17 45 51.51 (0.03)	−27 53 37.8 (0.4)	1612	L	+28	40
			1612	L	+69	50
			1612	R	+28	30
			1612	R	+69	60
M.....	17 46 12.09 (0.02)	−27 41 01.4 (0.1)	1612	L	−142	1350
			1612	L	−140	1300
			1612	L	−115	2910
			1612	L	−113	360
			1612	R	−142	1430
			1612	R	−140	1480
			1612	R	−115	3170
			1612	R	−113	410
N	17 46 22.09 (0.09)	−27 48 08.4 (0.8)	1612	L	+92	120
			1612	L	+108	160
			1612	R	+92	120
			1612	R	+108	170

[a] Maser spots that have intensities greater than 6 σ are tabulated.

the H_2O maser positions are superposed on the 6 cm continuum image from Figure 2. The spectra of the water masers are displayed in Figure 10.

Ten OH maser sites show 1612 MHz emission (all, except maser D, exhibit double-peaked profiles), indicating that these masers are probably associated with evolved stars. The four sites for which no 1612 MHz emission was detected are sources A, E, I, and K. In OH maser site A, a single 1667 MHz maser is detected at $v_{LSR} = +104$ km s^{-1}. The high velocity of this maser and the fact that it is not located near a known H II region indicates to us that this maser source is most likely associated with an evolved star. For the same reasons, maser site E, which exhibits 1667 MHz emission near +75 km s^{-1}, is also most likely an evolved star maser.

The velocity of OH maser site I, which exhibits 1665 MHz emission, is −19 km s^{-1}, which is quite close to that of the Sgr D molecular cloud/H II region. Furthermore, this source is projected at the edge of the Sgr D H II region (G1.13−0.10). For these reasons, this maser may be associated with a young stellar object. In addition, this OH maser is nearly coincident with H_2O maser source 2. The H_2O masers at this position have velocities ranging between −24 and −7 km s^{-1}, indicating that they may be located in a bipolar molecular outflow. It is well known that high-velocity molecular outflows traced by H_2O masers exist in other Galactic star-forming regions.

OH maser K exhibits 1665 MHz emission near +4 km s^{-1}. In addition, it is located only 8″ from source 1b of the continuum study. Unfortunately, this region was not

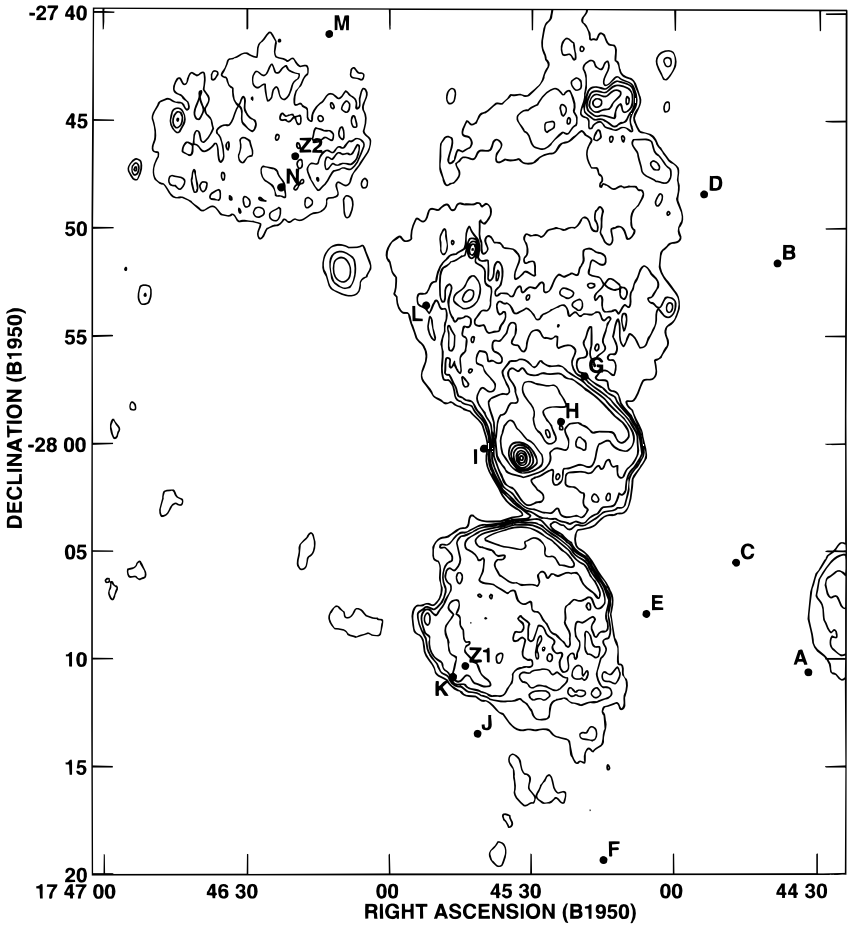

FIG. 7.—Contour 18 cm continuum image on which the positions of the OH maser sites are shown. In addition, the two 1720 MHz OH masers detected by Yusef-Zadeh et al. (1998) are indicated. These masers are labeled Z1 and Z2.

included in the H_2O maser study, so we do not know whether there are also H_2O masers associated with this source. Three attributes suggest that the OH masers in this region are associated with a young stellar object. They are (1) the lack of detectable 1612 MHz OH maser emission, (2) the proximity to a radio continuum source, and (3) the closeness of the maser velocities to the systemic velocity of the Sgr D H II region (G1.13−0.10). Because it cannot be determined whether continuum sources 1a and 1b, which lie well south of the main arc of the SNR G1.05−0.15, are actually associated with the Sgr D molecular cloud, the velocity of these continuum sources may indeed be closer to the velocity of maser source K than the -21 km s^{-1} systemic velocity of the ionized material in the main Sgr D H II region (G1.13−0.10).

The remaining H_2O maser, H_2O maser source 1, is projected only 4″ (0.15 pc) south of the peak of the brightest compact continuum source, source 3 (G1.12−0.10). Although this maser has a velocity of $+23$ km s^{-1}, which is over 40 km s^{-1} different from the Sgr D (G1.13−0.10) systemic velocity, its close proximity to continuum source 3 suggests it is associated with a young stellar object. The high velocity might be the result of the maser being located in a high-velocity molecular outflow. We detected no OH masers near this position. Thus this maser source may be similar to most of the H_2O masers detected by Mehringer, Palmer, & Goss (1993a) in Sgr B1. All but one of the Sgr B1 H_2O masers do not have OH counterparts, and for this reason Mehringer et al. (1993b) concluded that they are most likely associated with young stellar objects rather than evolved stars. A more complete survey of the Sgr D region for H_2O masers would be interesting, since, as is the case in Sgr B1, there may be many more H_2O masers associated with young stellar objects awaiting detection.

4. SUMMARY

We have carried out a program of VLA observations in order to gain a better understanding of the Sgr D (G1.13−0.10) massive star-forming region and the G1.05−0.15 SNR. The major results of this study are

1. Continuum observations at 6 and 18 cm show that the Sgr D H II region (G1.13−0.10) is dominated by a single compact source. This source is embedded in a 7′ diameter halo of ionized material. Numerous sources are located in the 36′ field. The rms electron number density of the extended component is 50 cm^{-3}, and it has a total mass of 3000 $M_\odot$. These values are similar to those previously determined for the extended ionized halos of Sgr B1 and Sgr B2. The SNR G1.05−0.15 is located 5′ south of the Sgr D H II region, and there is an SNR candidate, G1.4−0.1, located 15′ to the northeast of Sgr D (G1.13−0.10).
2. H_2CO absorption observations at 6 cm show that the molecular material in this region is clumpy. For example, in one cloud, the apparent optical depth is observed to vary by a factor of 10 over a projected distance of about 5 pc. In

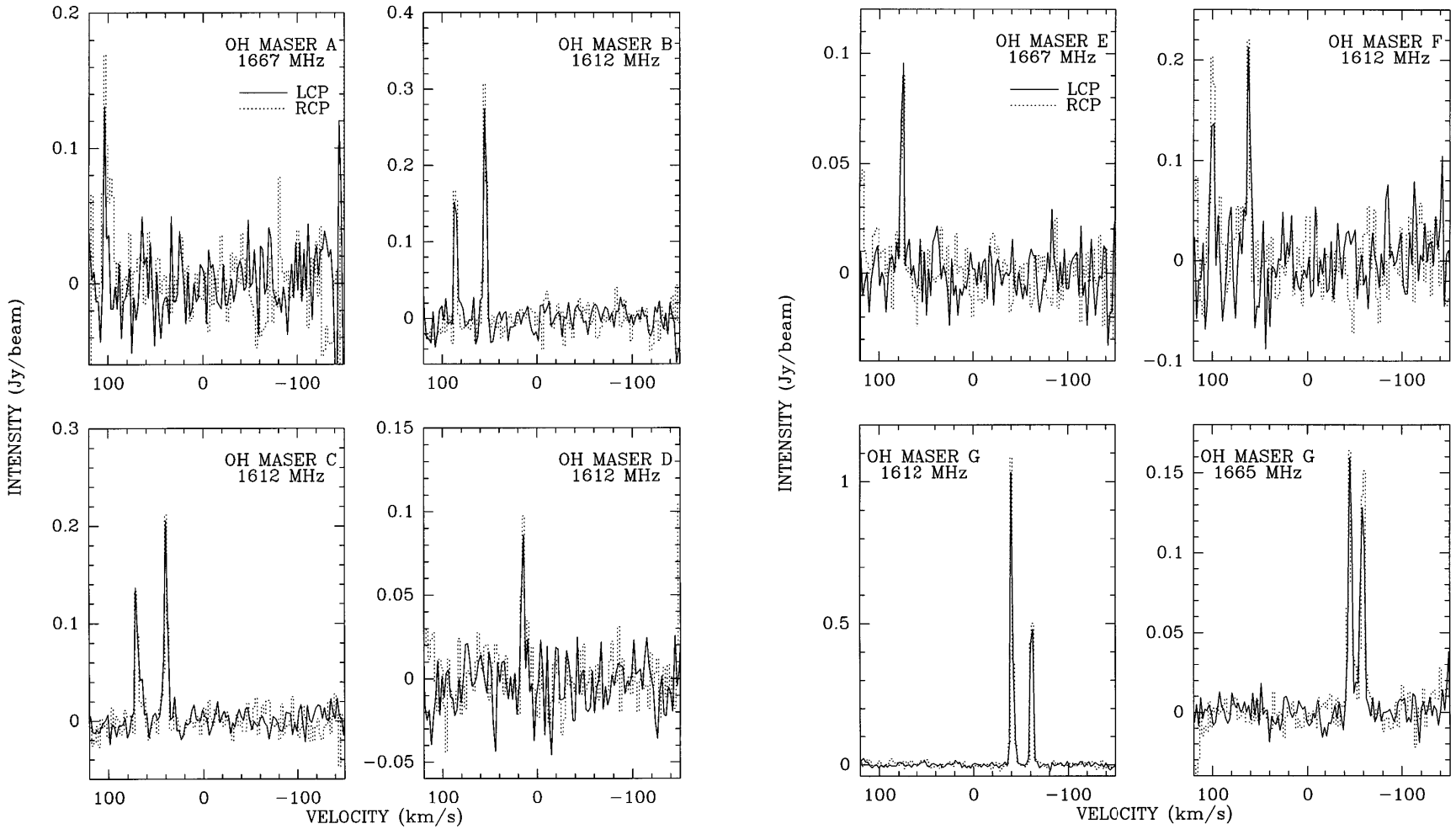

FIG. 8.—Spectra of the OH masers observed in this study. The solid, connected spectra and the dashed, histogram spectra represent the left and right circular polarizations, respectively.

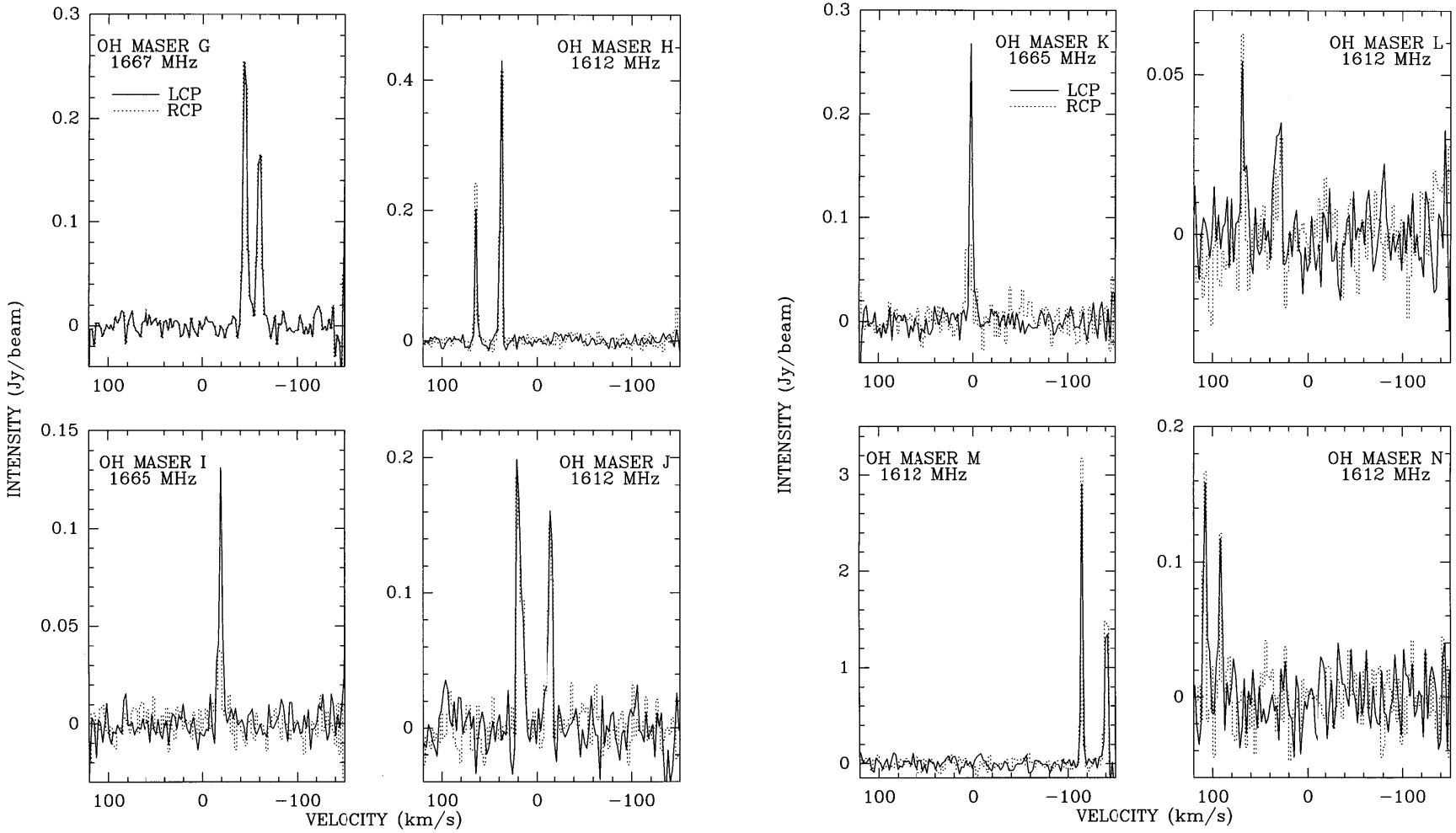

FIG. 8—*Continued*

TABLE 10

OBSERVATIONAL PARAMETERS OF H_2O MASERS TOWARD SGR D[a, b]

Source	α(B1950)	δ(B1950)	v_{LSR} (km s^{-1})	Flux Density (mJy)
1	17 45 32.24 (0.03)	−28 00 48.4 (0.3)	+22.9	130
			+24.2	120
2	17 45 39.29 (0.02)	−28 00 15.7 (0.2)	−23.9	7200
			−22.6	12,400
			−21.3	9800
			−20.0	4200
			−18.7	1100
			−16.0	900
			−9.5	1200
			−8.1	2100
			−6.8	1200

NOTE.—Units of right ascension are hours, minutes, and seconds, and units of declination are degrees, arcminutes, and arcseconds.

[a] Maser spots that have intensities greater than 6 σ are tabulated.

[b] The data have been Hanning smoothed, so that the actual spectral resolution is 2.6 km s^{-1}.

addition, the molecular clouds associated with the ionized material have narrow (<5 km s^{-1}) line widths, indicating that this complex is not located in the Galactic center region. Broad-line absorption features observed at highly positive velocities indicate that both the Sgr D H II region (G1.13−0.10) and the SNR G1.05−0.15 are located beyond the Galactic center.

3. OH and H_2O maser observations indicate that there are probably at least three sites of very recent star formation in this region. Furthermore, these data indicate that the H_2O masers may be located in high-velocity molecular outflows. In addition, the OH maser data indicate that there are at least 12 evolved stars in a 30′ diameter field containing Sgr D.

We thank A. D. Gray for helpful discussions and an anonymous referee for useful comments.

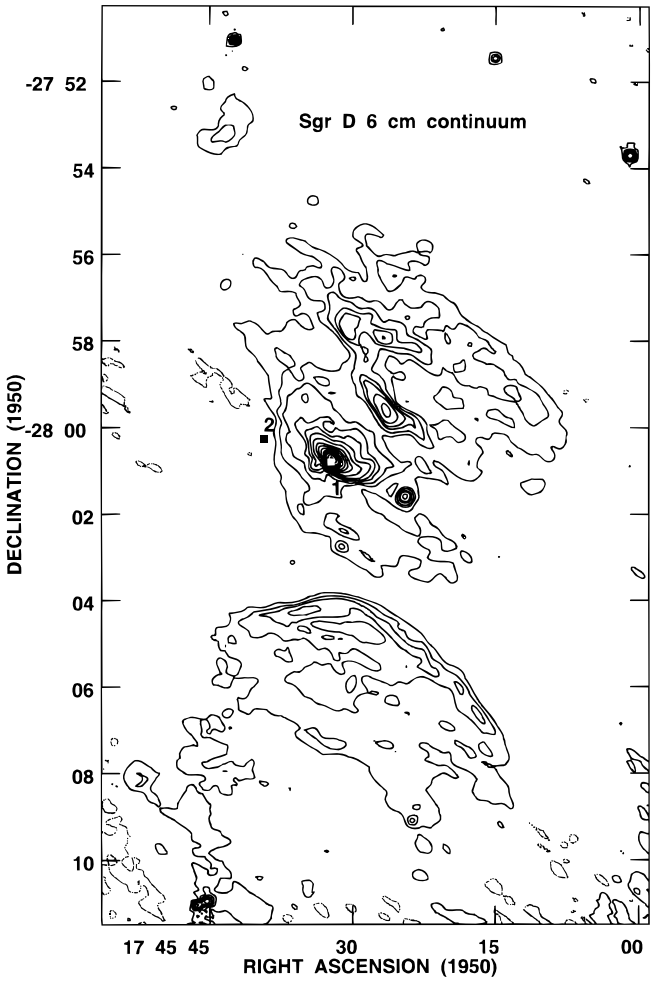

FIG. 9.—Contour 6 cm continuum image (identical to that in Fig. 2) on which the positions of the two H_2O masers detected in this study are shown.

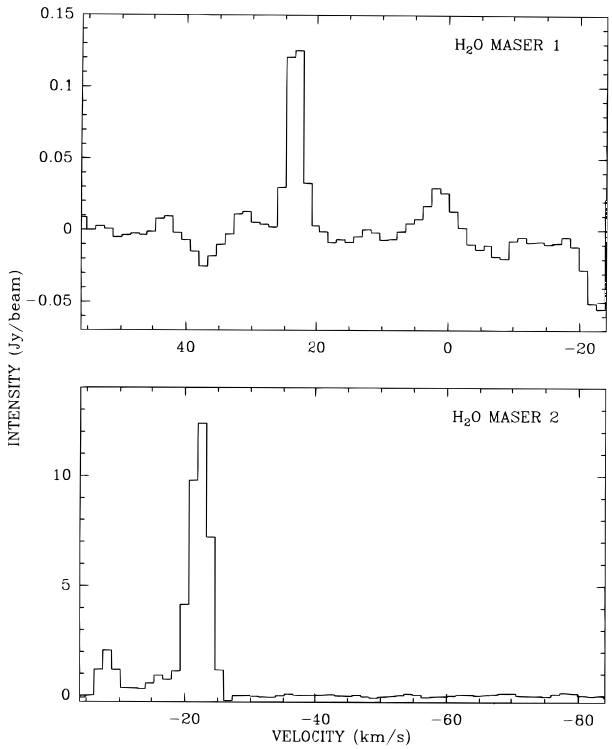

FIG. 10.—Spectra of the H_2O masers observed in this study. The spectra have been Hanning smoothed; thus the spectral resolution is two channels wide.

REFERENCES

Anantharamaiah, K. R., & Yusef-Zadeh, F. 1989, in IAU Symp. 136, The Center of the Galaxy, ed. M. Morris (Dordrecht: Kluwer), 159
Downes, D., Wilson, T. L., Bieging, J., & Wink, J. 1980, A&AS, 40, 379
Gray, A. D. 1994a, MNRAS, 270, 835
———. 1994b, MNRAS, 270, 847
Güsten, R. 1989, in IAU Symp. 136, The Center of the Galaxy, ed. M. Morris (Dordrecht: Kluwer), 89
Likkel, L. 1989, ApJ, 344, 350
Lis, D. C. 1991, ApJ, 379, L53
Lis, D. C., Menten, K. M., & Mehringer, D. M. 1998, in preparation
Liszt, H. 1992, ApJS, 82, 495
Mehringer, D. M., Palmer, P., & Goss, W. M. 1993a, ApJ, 402, L69
Mehringer, D. M., Palmer, P., Goss, W. M., & Yusef-Zadeh, F. 1993b, ApJ, 412, 684
Mehringer, D. M., Yusef-Zadeh, F., Palmer, P., & Goss, W. M. 1992, ApJ, 401, 168
Mezger, P. G., & Henderson, A. P. 1967, ApJ, 147, 471
Odenwald, S. F. 1989, in IAU Symp. 136, The Center of the Galaxy, ed. M. Morris (Dordrecht: Kluwer), 205
Odenwald, S. F., & Fazio, G. G. 1984, ApJ, 283, 601
Panagia, N. 1973, AJ, 78, 929
Panagia, N., & Walmsley, C. M. 1978, A&A, 70, 411
te Lintel Hekkert, P., Versteege-Hensel, H. A., Habing, H. J., & Wiertz, M. 1989, A&AS, 78, 399
Wadiak, E. J., Rood, R. T., & Wilson, T. L. 1988, ApJ, 324, 931
Wilson, W. J., & Barrett, A. H. 1972, A&A, 17, 385
Wood, D. O. S., & Churchwell, E. 1989, ApJS, 69, 831
Yusef-Zadeh, F., et al. 1998, in preparation